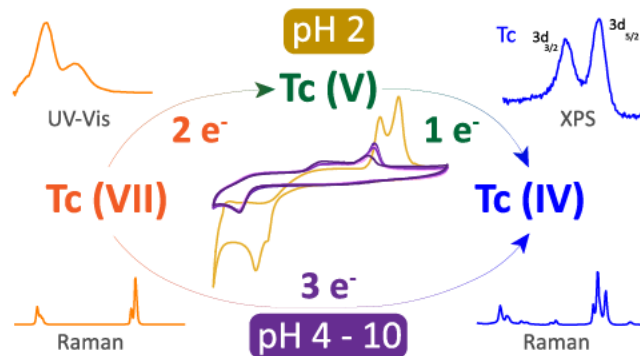


Exploring the Reduction Mechanism of $^{99}\text{Tc(VII)}$ in NaClO_4 : A Spectro-Electrochemical Approach

Diana M. Rodríguez, Natalia Mayordomo,* Andrés Parra-Puerto, Dieter Schild, Vinzenz Brendler, Thorsten Stumpf, and Katharina Müller*

ABSTRACT: Technetium (Tc) is an environmentally relevant radioactive contaminant whose migration is limited when Tc(VII) is reduced to Tc(IV). However, its reaction mechanisms are not well understood yet. We have combined electrochemistry, spectroscopy, and microscopy (cyclic voltammetry, rotating disk electrode, X ray photoelectron spectroscopy, and Raman and scanning electron microscopy) to study Tc(VII) reduction in non-complexing media: 0.5 mM KTcO_4 in 2 M NaClO_4 in the pH from 2.0 to 10.0. At pH 2.0, Tc(VII) first gains 2.3 ± 0.3 electrons, following Tc(V) rapidly receives 1.3 ± 0.3 electrons yielding Tc(IV). At pH 4.0–10.0, Tc(IV) is directly obtained by transfer of 3.2 ± 0.3 electrons. The reduction of Tc(VII) produced always a black solid identified as Tc(IV) by Raman and XPS. Our results narrow a significant gap in the fundamental knowledge of Tc aqueous chemistry and are important to understand Tc speciation. They provide basic steps on the way from non-complexing to complex media.



1. INTRODUCTION

Technetium (Tc, $Z = 43$), discovered by Sagré and Perrier in 1937,¹ is the lightest element with no stable isotopes. Among them, the most abundant is ^{99}Tc , a β particle emitter with a long half-life of 2.14×10^5 years. In the early 60s, the application as a clinical tracer of the metastable isotope, ^{99m}Tc (half-life of 6.007 h) was first published² and, since then, it has been used for the imaging of several organs such as the brain and the lungs.

Technetium might occur naturally within the earth crust originating from spontaneous fission of ^{238}U , neutron induced fission of ^{235}U , or interactions between molybdenum, ruthenium or niobium, and cosmic rays.³ However, the vast majority of the ^{99}Tc found on earth is a result of anthropogenic activity such as nuclear energy production and nuclear weapon testing^{3,4} as well as the decay product of ^{99m}Tc used in diagnostics.^{5,6} In a typical 1 GW nuclear power plant, 21 kg of ^{99}Tc (13.2×10^{15} Bq) are formed annually as a fission product; the global Tc production in 2007 was estimated to be 15.1×10^3 kg. Taking this as a rough average, in 2020, there were approximately 4.71×10^5 kg ^{99}Tc , equivalent to 2.963×10^{17} Bq, present on earth. The majority of Tc waste is still waiting for proper disposal in deep geological repositories that, combining engineered (e.g. vitrified waste, buffer and sealing materials, and borehole fillings) and geological barriers (host rock) will isolate the radioactive waste from the (hydro)biosphere for up to one million years.⁷

To ensure a safe storage, it is of utmost importance to understand Tc chemical behavior to assess its migration in water, which is strongly influenced by its aqueous speciation.⁸ Under oxidizing conditions, it occurs as pertechnetate, Tc(VII)O_4^- , an anion with high water solubility and low to no interaction with geochemical barriers.^{9,10} Consequently, an ingress of ground water to the repository under oxidizing conditions—as worst case scenario—will trigger the migration of Tc(VII) to the biosphere. There, it could easily get incorporated into the food chain causing health problems to animals and humans.^{3,7,11} Under reducing conditions, Tc(IV) is the most stable oxidation state, which commonly forms a solid, TcO_2 , with a low aqueous solubility ($\log K_{sp} = 8.17 \pm 0.05$ ¹²). Thus, the reduction of Tc(VII) to Tc(IV) is an effective strategy for technetium immobilization. Recently, several Fe(II) minerals have been studied in detail: iron sulfide in the form of pyrite and marcasite^{13–15} chukanovite,¹⁶ magnetite,^{17,18} or other common systems like layered double hydroxides¹⁹ trigger Tc(VII) reduction and then incorporate, precipitate, or adsorb Tc(IV).

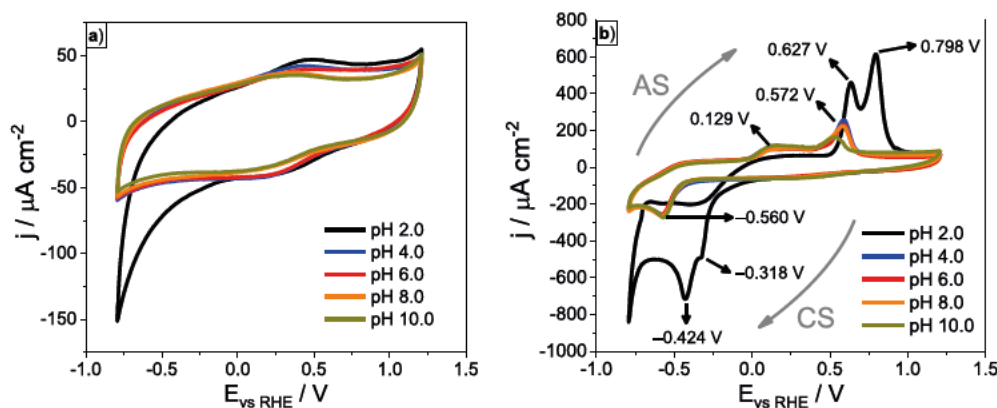


Figure 1. Cyclic voltammograms at 0.01 V s^{-1} scan rate in 2 M NaClO_4 under N_2 at different pH values (a) in the absence of Tc and (b) in the presence of 0.5 mM KTcO_4 . Gray arrows represent the voltage scan direction of the cathodic scan (CS) and the anodic scan (AS).

Despite the clear relevance of the reduction of Tc(VII) from an environmental and chemical point of view, more than 80 years after the discovery of technetium, its reduction mechanisms in water are not well understood yet.²⁰ Although several studies have been performed, especially in acidic media,^{21–23} it is not clear whether it proceeds in a direct three electron transfer or if there are intermediary oxidation states involved.^{24–26} Moreover, there is no systematic study of the effect of pH and ionic strength on the mechanism. There are also some contradictions observed in the literature. For example, Salaria et al.^{27,28} propose the reduction from Tc(VII) to Tc(III) passing through Tc(IV), whereas Grassi et al.²⁹ propose the reduction from Tc(VII) to Tc(IV) with the direct transfer of three electrons, and other authors suggest that the final product would be Tc(IV) with Tc(V) as an intermediary step.^{30–32} Moreover, it must be noted that all these previous studies use ions like Cl^- as background electrolytes that are well known to form complexes with technetium,^{12,33} invalidating such results for a formulation of redox mechanisms in pure water. This seriously hampers the modeling of technetium migration behavior in any compartment of geosphere or ecosphere.

In order to narrow this substantial gap in the understanding of technetium aqueous chemistry, we studied the reduction of Tc(VII) in sodium perchlorate (NaClO_4), a stable background electrolyte that does not form complexes with Tc(VII)³² and, in consequence, minimizes artefacts in reactive transport models for Tc in aqueous media. This will provide valuable reference data for more complex systems in the future. Experiments were performed at $2.0 \leq \text{pH} \leq 10.0$ in order to determine the effect of pH on the mechanism and the reaction products. To get comprehensive molecular understanding on Tc reduction chemistry, we combined electrochemical [cyclic voltammetry (CV) and rotating disk electrode (RDE)], spectroscopic (Raman and X ray photoelectron spectroscopy), and microscopic (scanning electron microscopy) methods.

2. MATERIALS AND METHODS

2.1. Sample Preparation. **2.1.1. Radiation Safety.** ^{99}Tc is a β particle emitter and should be handled only in a dedicated radiochemistry laboratory with specific radiation safety measures in place.

All solutions were prepared using $\text{K}^{99}\text{TcO}_4$ (Institute of Radio pharmaceutical Cancer Research at Helmholtz Zentrum Dresden Rossendorf), $\text{NaClO}_4 \times \text{H}_2\text{O}$ (purity $\geq 98\%$, PanReac AppliChem ITW Reagents), and Milli Q water (resistivity of $18.2 \text{ M}\Omega \text{ cm}$, Water

Purified). In general, 7 mL of 0.5 mM KTcO_4 solutions were prepared in 2 M NaClO_4 at pH 2.0, 4.0, 6.0, 8.0, and 10.0. The concentrations of both NaClO_4 and KTcO_4 were constant throughout the experiments. The pH was adjusted by adding small amounts (less than $10 \mu\text{L}$ in total) of HClO_4 or NaOH ; changes in ionic strength and viscosity were negligible. The pH was measured using a pH meter (pH3110, WTW) with a pH electrode (SI Analytics Blue Line) calibrated with standard pH buffers 4.006, 6.865, and 9.180 (WTW).

2.2. CV and RDE. The CV and RDE experiments were performed in an 884 Professional VA instrument from Metrohm using a three electrode set up in a glassy carbon electrode (diameter: $2 \pm 0.1 \text{ mm}$) as the working electrode (WE), platinum as the counter electrode (CE), and a Ag/AgCl (3 M KCl) reference electrode (RE); all potentials were converted to a reversible hydrogen electrode (RHE). The electrochemical surface area of the WE was determined as $0.035 \pm 0.001 \text{ cm}^2$ with a Randles–Sevcik analysis of $10 \text{ mM K}_3\text{Fe}(\text{CN})_6$ in 1.0 M KNO_3 using the diffusion coefficients reported in ref 34. The glassy carbon electrode was used in stationary mode for CV and in hydrodynamic mode for RDE. The experiments were performed under a normal atmosphere at $25 \text{ }^\circ\text{C}$, and all the solutions were purged with N_2 for 20 min before the measurement. The data obtained with the RDE were processed with the software AfterMath (version 1.5.9888, Pine Research) in order to obtain the limiting currents at the different angular velocities.

2.3. Spectro-Electrochemical Analysis. Figure S1 in the Supporting Information presents the in house built spectro electro chemical cell. The cell was placed inside a glovebox (GS Glovebox System GS050912; $<1 \text{ ppm O}_2$) represented by the orange colored line in Figure S1a. The cell holder was printed with a 3D printer (3DWOX 1, Sindoh). The quartz cell had the following outer dimensions: width $20 \times$ depth $10 \times$ height 30 mm and an optical path length of 5 mm . For the electrochemical reduction of Tc(VII), a three electrode arrangement was used. The WE was a glassy carbon rod (ALS Japan), the CE was a Pt wire (ALS Japan), and the RE was Ag/AgCl (3 M KCl) (ALS Japan). The electrodes were connected to a potentiostat (PGSTAT 101, Metrohm) outside the glovebox. An UV–vis spectrometer (AvaSpec ULS2048 StarLine, Avantes) was located outside the glovebox along with the lamp (AvaLight DH S BAL, Avantes), and both of them were connected to the cell holder using an optical fiber.

The spectro electrochemical experiments were carried out at $21 \text{ }^\circ\text{C}$. As a general procedure, the sample was placed inside the cell and it was stirred throughout the entire experiment with a 5 mm magnetic stirrer. A potential staircase was applied varying the potential 0.01 V every 4 min (e.g.: -0.480 V for 4 min , then -0.490 V again for 4 min , and etc. until -1 V vs Ag/AgCl or -0.790 V vs RHE). The starting potential of the staircase was -0.490 V versus Ag/AgCl at pH 2.0 and -0.620 V versus Ag/AgCl at pH 10.0. In parallel to the potential staircase, UV–vis spectra were continuously recorded (one spectrum every 30 s , i.e. 8 spectra per potential value) in the range from 200 to 1100 nm . The integration time was 10 ms , and a background

subtraction was performed using blanks of 2 M NaClO₄ at pH 2.0 and 10.0 depending on the sample. The 8 spectra obtained for each potential step were averaged in order to reduce the noise.

2.4. Solid Analysis. After the complete reduction of Tc(VII) in the spectro electrochemical cell at pH 2.0, a black solid was accumulated on the WE. The electrode was taken outside the solution, and when it got dry, the solid detached itself immediately and was collected for further study. The reduction in the spectro electrochemical cell was repeated at pH 10.0 obtaining again a solid accumulated on the electrode that was also harvested. Both solid samples were studied by Raman microscopy, with a second batch of the solid obtained at pH 2.0 also being analyzed using scanning electron microscopy with energy dispersive X ray spectroscopy (SEM–EDX) and X ray photoelectron spectroscopy (XPS). Experimental conditions for Raman measurements³⁵ and for SEM–EDX and XPS¹⁵ are described elsewhere and detailed in the [Supporting Information](#).

The supernatant was analyzed by liquid scintillation counting (1414 LSC WinSpectral α/β Wallac, PerkinElmer; detection limit: 25 cpm. Measuring time: 10 min) finding that only 80 Bq out of the initial 321 000 Bq remained in the solution, meaning that all Tc(VII) was reduced to the black Tc solid.

3. RESULTS AND DISCUSSION

3.1. Electrochemical Characterization, CV, and RDE.

[Figure 1](#) shows the cyclic voltammograms of NaClO₄ solutions in the absence ([Figure 1a](#)) and presence of Tc ([Figure 1b](#)) in the pH range from 2.0 to 10.0.

As mentioned before, unlike chloride (Cl[−]), perchlorate (ClO₄[−]) does not form complexes with technetium.¹² In addition to that, the voltammogram of NaClO₄ ([Figure 1a](#)) shows only very small peaks close to 0.1 V versus RHE and some hydrogen evolution reaction potentials below −0.625 V at pH 2.0. In the presence of Tc, the voltammograms clearly change. Thus, the peaks in [Figure 1b](#) indicate the course of different oxidation states of technetium within the cycling voltammograms.

Two different Tc reduction behaviors can be spotted in the CVs depending on the pH in the cathodic scan. At pH 2.0, the system clearly shows two peaks during the reduction. A small peak at −0.318 V suggests the formation of an intermediary oxidation state, followed by a second reduction peak observed at −0.424 V. In contrast, at pH 4.0–10.0, one single cathodic peak (CP) at −0.560 V indicates a direct Tc(VII) reduction.

The voltammograms in [Figure 1b](#) show two anodic peaks despite the pH value, that is, the formation of two Tc oxidation states. The potential of the reactions depends on the pH alike the reduction: while at pH 4.0–10.0, they behave in a similar way (anodic peaks at 0.129 and 0.570 V), and the peaks at pH 2.0 are shifted to more positive values (0.627 and 0.789 V).

Although the CVs provide already an idea on the mechanism of the Tc reduction and oxidation, they cannot be used for the determination of the exact amount of electrons transferred due to the irreversibility of the process. For an improved understanding of the redox processes occurring, we combine CV at different scan rates and the RDE technique to apply the Randles–Sevcik and Levich equations for electrochemical data analysis. A full description of the equations and how to interpret them is defined as follows.

On one hand, by changing the scan rate of the CV, the peak currents can be analyzed with the Randles–Sevcik equation ([eq 1](#)).^{36,37} It is assumed that all Tc remains dissolved and there is no precipitation or deposition on the electrode.

$$I_p = 2.69 \times 10^5 n^{3/2} A c D^{1/2} u^{1/2} \quad (1)$$

where I_p is the peak current (A), n is the number of electrons transferred, A is the area of the electrode (cm²), c is the analyte concentration (mol cm^{−3}), D is the diffusion coefficient (cm² s^{−1}), and u is the CV scan rate (V s^{−1}). The terms n , A , c , and D do not change here and can be grouped along with 2.69×10^5 in a new term Y . Therefore, [eq 1](#) can be rewritten as [eq 2](#).

When I_p is plotted versus $u^{1/2}$ (Randles–Sevcik plot), a straight line with slope Y is obtained.

$$I_p = Y u^{1/2} \quad (2)$$

On the other hand, using a RDE, the diffusion coefficients and the number of electrons can be determined. RDE is an experimental technique, in which the WE rotates on its own axis creating a laminar flow of the solution toward the electrode, improving the mass transport.³⁸ Such flow can be controlled by the angular velocity of the electrode, and the behavior of the current is modeled using the Levich equation ([eq 3](#)).³⁸

$$I_L = (0.620)nFA\nu^{-1/6} D^{2/3} c\omega^{1/2} \quad (3)$$

where I_L is the limiting current (A), which is the mass transport limited current obtained at the different rotation speed, n is the number of electrons transferred, F is the Faraday constant (96 485.3329 C mol^{−1}), A is the area of the electrode (cm²), ν is the kinematic viscosity of the electrolyte (cm² s^{−1}), D is the diffusion coefficient of the species under study, that is, the electroactive species (cm² s^{−1}), c is the analyte concentration (mol cm^{−3}), and ω is the angular velocity of the RDE (rads^{−1}). Alike Randles–Sevcik equation, n , A , ν , D , and c can be grouped along with $0.620 F$ in B (Levich constant), and [eq 3](#) can be summarized as [eq 4](#).

$$I_L = B\omega^{1/2} \quad (4)$$

When plotting I_L versus $\omega^{1/2}$ (Levich plot), B is obtained from the slope of a linear fit and is used to determine the number of electrons transferred n or the diffusion coefficient D . In our system, we have approximated ν by 8.90×10^{-3} cm² s^{−1} corresponding to the kinematic viscosity of 2 M NaClO₄ in water.³⁹ The Tc concentration (0.5 mM) was low enough to neglect its effect on the viscosity.

Combining the slopes of the regression lines from the Randles–Sevcik and the Levich equations, two equations ([eqs 5](#) and [6](#)) are obtained for two unknown variables (D —the diffusion coefficient of Tc in 2 M NaClO₄ and n)

$$Y = 2.69 \times 10^5 A c D^{1/2} n^{3/2} \quad (5)$$

$$B = 0.620 F c A \nu^{-1/6} D^{2/3} n \quad (6)$$

Solving this equation system, [eqs 7](#) and [8](#) were obtained, directly yielding D and n , respectively

$$D = \left(\frac{\alpha E}{B} \right)^2 \quad (7)$$

$$n = \frac{Y}{\alpha D^{3/2}} \quad (8)$$

with $\alpha = 0.620 F c A \nu^{-1/6}$, $E = (Y/\beta)^{3/2}$, and $\beta = 2.69 \times 10^5 A c$.

Since the reduction of Tc(VII) in NaClO₄ appears to follow the same mechanism throughout the pH range 4.0–10.0 according to [Figure 1b](#), we selected pH 2.0 and pH 10.0 for the RDE experiments to encompass the working pH range by

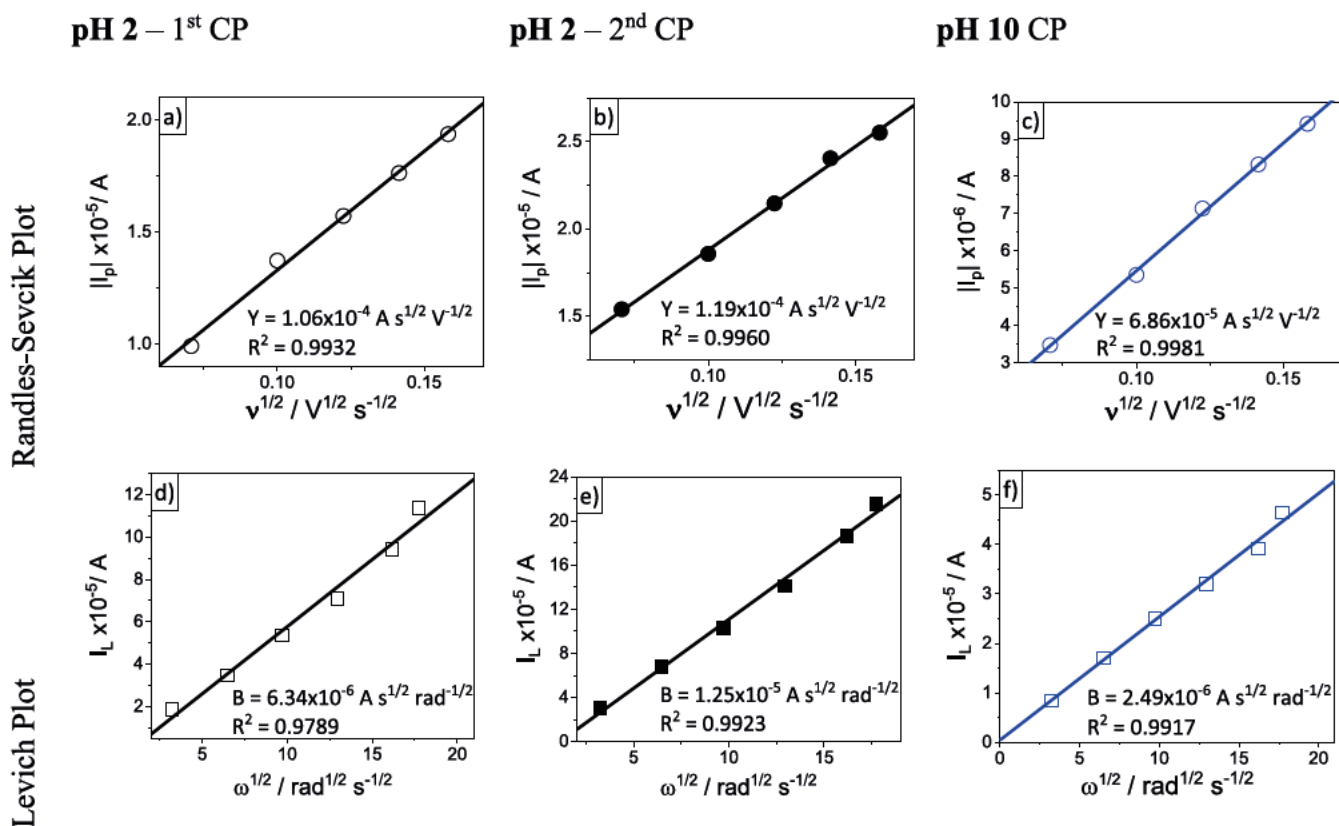


Figure 2. (Circles) Randles–Sevcik and (squares) Levich plots of 0.5 mM KTCO_4 in 2 M NaClO_4 at different pH values. (a,d) First CP at pH 2.0 (-0.318 V). (b,e) Second CP at pH 2.0 (-0.424 V) (c,f) CP at pH 10.0 (-0.560 V). Y and B are the Randles–Sevcik and Levich slopes (eqs 5 and 6 respectively).

measuring the two extremes. The reduction curves of the systems at different angular velocities as well as the cyclic voltammograms at different scan rates are presented in Figures S2 and S3 in the Supporting Information. Figure 2 shows the Randles–Sevcik and Levich plots of Tc at pH 2.0 and pH 10.0. There is a clear linear correlation between I_L and $\omega^{1/2}$ as well as for I_p and $v^{1/2}$, and, therefore, the values for the slopes B and Y were replaced in eqs 5 and 6 to obtain D and n at both pH values.

Table 1 summarizes the results of the electrochemical analysis.

We have found that at pH 2.0, the reduction of Tc(VII) begins with the transfer of 2.3 ± 0.3 electrons, yielding Tc(V) as an intermediary oxidation state that subsequently gains further 1.3 ± 0.3 electrons to become Tc(IV). At pH 10.0, the reduction of Tc(VII) is direct with the transfer of 3.2 ± 0.3 electrons to produce Tc(IV). The uncertainties in the number of errors were calculated using the error propagation method described elsewhere.⁴⁰

The electrochemical behavior displayed at pH 2.0 is in good agreement with the Latimer diagram of Tc under acidic conditions,⁴¹ where Tc(VI) is postulated as an intermediary oxidation state during the reduction from Tc(VII) to Tc(IV). However, as Tc(VI) is unstable in water, a rapid disproportionation to Tc(VII) and Tc(V) takes place.^{25,27,29} This supports electrochemical analysis (Table 1), suggesting that the small peak at -0.318 V at pH 2.0 is Tc(V). The potential shift with pH related to Tc(IV) formation (-0.424 V for pH 2 and -0.560 V for pH values 4.0, 6.0, 8.0, and 10.0) can be related to the difference in the pH, as it occurs; for example, with

Table 1. Reduction Mechanism of Tc(VII) in NaClO_4 at pH 2.0 and pH 4.0–10.0 in Their Respective CP and the Associated Reduction Potential Versus RHE (E_{vsRHE})^a

CP	pH		
	2.0	4.0	10.0
1	$\text{Tc(VII)} + 2.3 \pm 0.3 e^- \rightarrow \text{Tc(V)}$, $D = 3.92 \times 10^{-5} \text{ cm}^2 \text{ s}^{-1}$, $E_{\text{vsRHE}} = 0.318 \text{ V}$	$\text{Tc(VII)} + 3.2 \pm 0.3 e^- \rightarrow \text{Tc(IV)}$, $D = 5.75 \times 10^{-6} \text{ cm}^2 \text{ s}^{-1}$, $E_{\text{vsRHE}} = 0.560 \text{ V}$	
2	$\text{Tc(V)} + 1.3 \pm 0.3 e^- \rightarrow \text{Tc(IV)}$, $D = 2.41 \times 10^{-4} \text{ cm}^2 \text{ s}^{-1}$, $E_{\text{vsRHE}} = 0.424 \text{ V}$		

^a n and D were calculated with eqs 7 and 8.

manganese where the reduction from Mn(VII)O_4^- to Mn(IV)O_2 has a standard potential of 1.7 V at acidic pH and 0.60 V at alkaline pH, according to Mn Latimer diagrams.²⁵

The diffusion coefficients of the electroactive Tc species in NaClO_4 at pH 2.0 were determined as $3.92 \times 10^{-5} \text{ cm}^2 \text{ s}^{-1}$ for Tc(VII) and $2.41 \times 10^{-4} \text{ cm}^2 \text{ s}^{-1}$ for Tc(V). At pH 10.0, the diffusion coefficient of Tc(VII) is $5.75 \times 10^{-6} \text{ cm}^2 \text{ s}^{-1}$. The starting Tc oxidation state at both pH 2.0 and pH 10.0 is Tc(VII), and therefore, it is clear that pertechnetate is the electroactive species of the first CP at both pH values. Previous studies on Tc diffusion coefficients in aqueous solution are extremely limited, and no value could be found in the presence of a salt that remotely resembles NaClO_4 (like KClO_4 or NaBrO_4). For the sake of comparison, the values obtained in our work were contrasted against the diffusion coefficients of Tc in bentonite,⁴² where it was reported that the diffusion

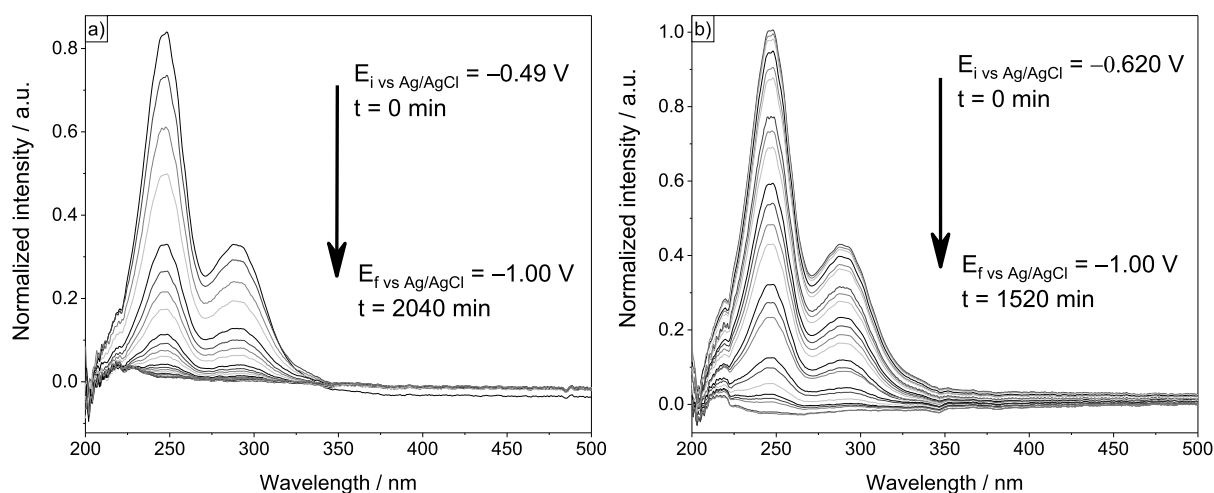


Figure 3. UV-vis spectra measured during the electrochemical reduction of 0.5 mM Tc(VII)O_4^- in 2 M NaClO_4 . (a) pH 2.0. (b) pH 10.0.

coefficient of pertechnetate decreases as pH increases, which is in good agreement with our findings with the RDE for the reduction mechanism of Tc(VII) (Table 1).

The oxidation mechanism could not be established because it was not possible to stabilize the reduced Tc aqueous species—theoretically Tc(IV) —at the beginning of the experiment. As it will be shown in section **Solid Analysis**, the complete reduction of Tc(VII) led to the formation of a solid deposited on the WE, making it impossible to apply the electrochemical analysis presented in this section as it is only feasible for species in solution. It is worth explaining that this issue did not affect the determination of the reduction mechanism because both the RDE and the CV experiments were fast enough to avoid the precipitation of the reduced Tc. However, the complete reduction of Tc(VII) necessary to start the RDE experiment for the oxidation takes several hours, giving enough time for the deposition of the reduced Tc solid. We can interpret that the second anodic peak (0.798 V at pH 2.0 and around 0.570 V at pH 4.0–10.0) in Figure 1b corresponds to the formation of Tc(VII) , as this is the highest stable oxidation state in solution for technetium.

3.2. In Situ Spectro-Electrochemical Analysis of Tc(VII) Reduction. Spectro electrochemical experiments were performed to follow the electrochemical reduction of Tc(VII)O_4^- in NaClO_4 at both pH 2.0 and 10.0. The collected UV-vis spectra are shown in Figure 3. As expected, both spectral data sets display at the beginning of the experiments the characteristic signals of TcO_4^- at 247 and 289 nm.²⁴ With the application of the potential staircase, the intensity of these features gradually decreases until both bands finally disappear at the last potential steps, indicating full reduction of Tc(VII) . The process was identical at both pH 2.0 and 10.0 (Figure 3a,b).

The complete reduction of Tc(VII) yielded a black solid deposited on the WE, regardless of the sample pH. Taking into account that UV-vis spectra confirm the lack of Tc(IV) chloride species with absorption at 234 and 338 nm⁴³ and that Tc(IV) is the final reduction product (Table 1), most likely the formed solid is a Tc(IV)-O species.

The spectroscopic behavior depicted in Figure 3b is in good agreement with the findings of the electrochemical analysis at pH 10.0 with no intermediary oxidation state between Tc(VII) and Tc(IV) during the reduction. Therefore, the occurrence of a Tc signal different from those of Tc(VII) was not expected.

However, no spectroscopic evidence of the existence of the Tc(V) species suggested by the electrochemical analysis at pH 2.0 was found. This can be due to an extremely fast transition from Tc(V) to Tc(IV) or simply because the Tc(V) species is not active in the UV-vis range or its absorption coefficient is too low.

3.3. Solid Analysis. In order to confirm the chemical identity of the solid obtained after the complete reduction of Tc(VII)O_4^- , Raman spectroscopy, XPS, and SEM-EDX were performed. The Raman spectra of the solids at pH 2.0 and 10.0 are shown in Figure 4.

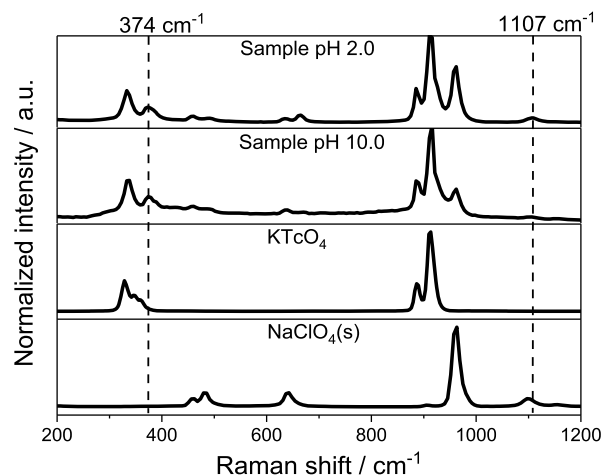


Figure 4. Raman spectra of the black solid obtained after the total reduction of 0.5 mM KTcO_4 in 2 M NaClO_4 at pH 2.0 and 10.0 in the spectro electrochemical cell. The Raman spectra of KTcO_4 and NaClO_4 have been added for comparison.

It can be observed that the Raman spectra are identical for both samples, indicating that the chemical identity of the solids at both pH values is the same, supporting the results in Table 1. The spectra of the samples were compared with the spectra of KTcO_4 and NaClO_4 . The bands at 458, 632, 666, and 960 cm^{-1} were attributed to sodium perchlorate⁴⁴ recrystallized on the WE along with the technetium solid.

The band at 330 cm^{-1} is assigned to Tc-O vibrations by comparison with the KTcO_4 spectra.^{45,46} However, it is worth mentioning that according to the literature,^{43,47,48} the Tc-Cl

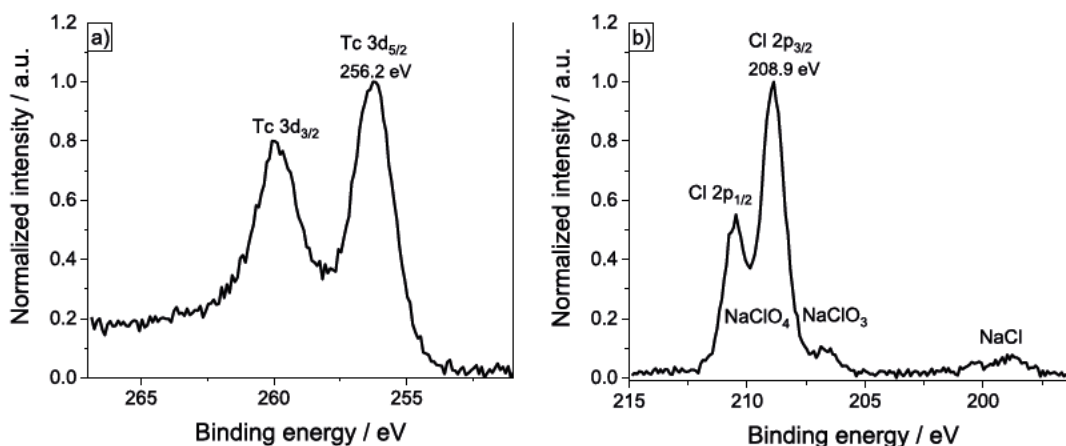


Figure 5. XPS spectra of the reduced Tc solid. (a) Tc 3d, (b) Cl 2p.

bond presents two bands at 332 and 342 cm^{-1} . While no band around 340 cm^{-1} is present in the spectra of the samples, the bands appearing at 885 and 913 cm^{-1} are characteristic of the TcO_4^- structure corresponding to Tc–O vibrations.^{45,46} Therefore, the band at 330 cm^{-1} is also assigned to the Tc–O vibration and no evidence of Tc–Cl bonding is present in the Raman spectra. This confirms that no interaction between Tc and chlorine species took place during the reduction.

Two bands at 374 and 1107 cm^{-1} remain unidentified after this assignment. Since the initial components of the samples were KTcO_4 , NaClO_4 , and water, these two remaining bands can be tentatively assigned to the reduced Tc solid that would be Tc(IV) according to the electroanalysis (Table 1). Previous works^{49,50} have reported a signal at 877 cm^{-1} for TcO_2 that does not appear in the Raman spectra of our samples. There is a possibility that this signal is overlapped by the band at 885 cm^{-1} , but as no reports for signals at 374 and 1107 cm^{-1} have been found for TcO_2 , we refrain from characterizing the solid samples as technetium dioxide.

In order to confirm the oxidation state of technetium in the solid, XPS and SEM–EDX were applied. The XPS spectra of the solid evaluated in Tc 3d and Cl 2p are presented in Figure 5.

The Tc 3d spectrum (Figure 5a) shows an intense Tc 3d_{5/2} peak at 256.2 eV assigned to Tc(IV) since it is close to the reference value for TcO_2 (256.8 eV⁵¹). NaClO_4 was present during the recording of the XPS spectra of the sample because no further separation or purification of the solid was performed after the reduction of Tc(VII) (see Solid Analysis in the Experimental Section). The Cl 2p_{3/2} elemental line of NaClO_4 is observed at 208.9 eV binding energy in accordance with its reference at 208.9 eV.⁵² Since NaClO_4 degrades under X ray irradiation and the charge of the sample surface caused by the XPS measurement will change slowly during degradation, charge referencing of elemental lines is not reliable if high degradation of NaClO_4 occurs. This was avoided by using monochromatic Al K α X rays, larger analysis area, and short acquisition time. Small portions of chlorite and chloride, that is, the degradation products, are detected at the Cl 2p spectrum (Figure 5b), making the results presented reliable despite the presence of NaClO_4 .

Even though XPS cannot be used to establish the structure of the technetium compound, the oxidation state can be unequivocally assigned as Tc(IV). Therefore, the bands found at 374 and 1107 cm^{-1} in the Raman spectra correspond to

Tc(IV). To our knowledge, apart from the band at 877 cm^{-1} for TcO_2 ,⁴³ no other Raman signals for Tc(IV) have been reported before, making the results of this paper very relevant for the identification of Tc(IV) in other applications, for example, Tc retention studies by minerals.

The SEM–EDX analysis is presented in Figure S4 in the Supporting Information. The morphology of the sample depicted in the micrographs shows three regions clearly separated: (1) mainly Na, Cl, and O, (2) almost completely Tc and O, and (3) indium from the foil on which the sample was prepared. This is consistent with the fact that ClO_4^- had no interaction with Tc and the solid obtained corresponds only to a reduced Tc species bonded to O.

4. CONCLUSIONS

The reduction of Tc(VII) in non complexing media (NaClO_4) has been studied for the first time using spectro electrochemical methods and electrochemical analysis, combined with other spectroscopic and microscopic techniques.

The electrochemical results show that the reaction mechanism depends on the pH. By applying Randles–Sevcik and Levich equations, the number of electrons during electrochemical analysis was determined. At pH 2.0, the reduction occurs in two steps with the initial gain of 2.3 ± 0.3 electrons by Tc(VII) to obtain Tc(V), which subsequently receives 1.3 ± 0.3 electrons to form Tc(IV). At pH 4.0–10.0, Tc(VII) is directly reduced to Tc(IV) with the transfer of 3.2 ± 0.3 electrons. The electrochemical reduction of Tc(VII) in NaClO_4 was followed in parallel with UV–vis absorption spectroscopy. Even though no spectroscopic evidence of intermediate Tc(V) could be obtained, UV–vis showed the absence of Tc(IV)–chloride species. After the total reduction of Tc(VII) at both pH 2.0 and 10.0, a black solid was formed. Raman spectroscopy confirmed that both solids had the same chemical identity despite the initial pH value, whereas SEM–EDX analysis proves that the solid only consists of Tc and O. XPS analysis identified the solids as Tc(IV) and agrees with the obtained CV results and the electrochemical analysis.

In addition to an accurate determination of the electrons transferred in the reduction process depending on the pH, this study has also yielded two Raman signals at 374 and 1107 cm^{-1} that correspond to the Tc(IV) species formed after the total reduction of Tc(VII). Such Raman features will be relevant to specific questions in environmental engineering for the identification of Tc(IV) compounds that are the

products of the reductive immobilization of Tc(VII) by common minerals and could only be identified by the use of more expensive spectroscopies.

This work presents fundamental data to understand Tc redox chemistry and its dependence on pH under the simplest aqueous conditions, that is, in a non complexing media.

Both results and methodology applied in the electrochemical analysis will serve as valuable references for further studies to identify Tc redox chemistry in complex systems, for example, in the presence of inorganic and organic ligands. These fundamental studies are essential for a realistic and broad picture of the Tc chemical redox and complexation behavior. A basic Tc chemical understanding will also provide a direct impact on environment protection by enhancing Tc remediation strategies in contaminated areas as well as for the safety assessment of nuclear waste repositories.

Furthermore, this work is also the first step toward a future development of spectro electrochemical techniques. We envision the development of spectro electrochemistry couplings to characterize the structure of redox active species at different oxidation states, which will be helpful not only for Tc but also for other redox active elements whose chemical behavior is still to be fully defined.

ASSOCIATED CONTENT

Supporting Information

The Supporting Information is available free of charge at <https://pubs.acs.org/doi/10.1021/acs.inorgchem.2c01278>.

In house built spectro electrochemical cell; reduction curves; CVs at different scan rates; and SEM–EDX experimental description of Tc solid analysis (PDF)

AUTHOR INFORMATION

Corresponding Authors

Natalia Mayordomo – Institute of Resource Ecology, Helmholtz Zentrum Dresden Rossendorf e.V., 01328 Dresden, Germany; orcid.org/0000-0003-4433-9500; Phone: +49 351 260 2076; Email: n.mayordomo@hzdr.de

Katharina Müller – Institute of Resource Ecology, Helmholtz Zentrum Dresden Rossendorf e.V., 01328 Dresden, Germany; orcid.org/0000-0002-0038-1638; Phone: +49 351 260 2439; Email: k.mueller@hzdr.de

Authors

Diana M. Rodríguez – Institute of Resource Ecology, Helmholtz Zentrum Dresden Rossendorf e.V., 01328 Dresden, Germany

Andrés Parra Puerto – Department of Chemistry, Imperial College London, SW7 2AZ London, U.K.; orcid.org/0000-0002-1131-1168

Dieter Schild – Institute for Nuclear Waste Disposal, Karlsruhe Institute of Technology (KIT), 76344 Eggenstein Leopoldshafen, Germany; orcid.org/0000-0001-6034-8146

Vinzenz Brendler – Institute of Resource Ecology, Helmholtz Zentrum Dresden Rossendorf e.V., 01328 Dresden, Germany; orcid.org/0000-0001-5570-4177

Thorsten Stumpf – Institute of Resource Ecology, Helmholtz Zentrum Dresden Rossendorf e.V., 01328 Dresden, Germany

Notes

The authors declare no competing financial interest.

ACKNOWLEDGMENTS

We are very grateful to Susana Jiménez and Stephan Weiß for their help in the lab. We acknowledge the German Federal Ministry for Economic Affairs and Climate Action (former German Federal Ministry of Economic Affairs and Energy) for the VESPA II joint project (02E11607B).

REFERENCES

- (1) Perrier, C.; Segrè, E. Radioactive Isotopes of Element 43. *Nature* 1937, 140, 193–194.
- (2) Herbert, R.; Kulke, W.; Shepherd, R. T. The Use of Technetium 99m as a Clinical Tracer Element. *Postgrad. Med. J.* 1965, 41, 656–662.
- (3) Meena, A. H.; Arai, Y. Environmental Geochemistry of Technetium. *Environ. Chem. Lett.* 2017, 15, 241–263.
- (4) Momoshima, N.; Sayad, M.; Yamada, M.; Takamura, M.; Kawamura, H. Global Fallout Levels of ^{99}Tc and Activity Ratio of $^{99}\text{Tc}/^{137}\text{Cs}$ in the Pacific Ocean. *J. Radioanal. Nucl. Chem.* 2005, 266, 455–460.
- (5) Guérin, B.; Tremblay, S.; Rodrigue, S.; Rousseau, J. A.; Dumulon Perreault, V.; Lecomte, R.; van Lier, J. E.; Zyuzin, A.; van Lier, E. J. Cyclotron Production of $^{99\text{m}}\text{Tc}$: An Approach to the Medical Isotope Crisis. *J. Nucl. Med.* 2010, 51, 13N–16N.
- (6) Jurisson, S.; Gawenis, J.; Landa, E. R. Sorption of $^{99\text{m}}\text{Tc}$ Radiopharmaceutical Compounds by Soils. *Health Phys.* 2004, 87, 423.
- (7) Icenhower, J. P.; Qafoku, N. P.; Zachara, J. M.; Martin, W. J. The Biogeochemistry of Technetium: A Review of the Behavior of an Artificial Element in the Natural Environment. *Am. J. Sci.* 2010, 310, 721–752.
- (8) Lear, G.; McBeth, J. M.; Boothman, C.; Gunning, D. J.; Ellis, B. L.; Lawson, R. S.; Morris, K.; Burke, I. T.; Bryan, N. D.; Brown, A. P.; Livens, F. R.; Lloyd, J. R. Probing the Biogeochemical Behavior of Technetium Using a Novel Nuclear Imaging Approach. *Environ. Sci. Technol.* 2010, 44, 156–162.
- (9) Lieser, K. H.; Bauscher, C. Technetium in the Hydrosphere and in the Geosphere. I Chemistry of Technetium and Iron in Natural Waters and Influence of the Redox Potential on the Sorption of Technetium. *Radiochim. Acta* 1987, 42, 205–214.
- (10) Masters Waage, N. K.; Morris, K.; Lloyd, J. R.; Shaw, S.; Mosselmans, J. F. W.; Boothman, C.; Bots, P.; Rizoulis, A.; Livens, F. R.; Law, G. T. W. Impacts of Repeated Redox Cycling on Technetium Mobility in the Environment. *Environ. Sci. Technol.* 2017, 51, 14301–14310.
- (11) Corkhill, C. L.; Bridge, J. W.; Chen, X. C.; Hillel, P.; Thornton, S. F.; Romero Gonzalez, M. E.; Banwart, S. A.; Hyatt, N. C. Real Time Gamma Imaging of Technetium Transport through Natural and Engineered Porous Materials for Radioactive Waste Disposal. *Environ. Sci. Technol.* 2013, 47, 13857–13864.
- (12) Grenthe, I.; Gaona, X.; Plyasunov, A. V.; Rao, L.; Runde, W. H.; Grambow, B.; Konings, R. J. M.; Smith, A. L.; Moore, E. E. *Second Update on the Chemical Thermodynamics of Uranium, Neptunium, Plutonium, Americium and Technetium*; OECD Nuclear Energy Agency Data Bank: Boulogne Billancourt: France, 2020.
- (13) Rodríguez, D. M.; Mayordomo, N.; Scheinost, A. C.; Schild, D.; Brendler, V.; Müller, K.; Stumpf, T. New Insights on the $^{99}\text{Tc(VII)}$ Removal by Pyrite: A Spectroscopic Approach. *Environ. Sci. Technol.* 2020, 54, 2678–2687.
- (14) Huo, L.; Xie, W.; Qian, T.; Guan, X.; Zhao, D. Reductive Immobilization of Per technetate in Soil and Groundwater Using Synthetic Pyrite Nanoparticles. *Chemosphere* 2017, 174, 456–465.
- (15) Rodríguez, D. M.; Mayordomo, N.; Schild, D.; Shams Aldin Azzam, S.; Brendler, V.; Müller, K.; Stumpf, T. Reductive Immobilization of $^{99}\text{Tc(VII)}$ by FeS_2 : The Effect of Marcasite. *Chemosphere* 2021, 281, 130904.

- (16) Schmeide, K.; Rossberg, A.; Bok, F.; Shams Aldin Azzam, S.; Weiss, S.; Scheinost, A. C. Technetium Immobilization by Chukanovite and Its Oxidative Transformation Products: Neural Network Analysis of EXAFS Spectra. *Sci. Total Environ.* **2021**, *770*, 145334.
- (17) Yalçıntaş, E.; Scheinost, A. C.; Gaona, X.; Altmaier, M. Systematic XAS Study on the Reduction and Uptake of Tc by Magnetite and Mackinawite. *Dalton Trans.* **2016**, *45*, 17874–17885.
- (18) Marshall, T. A.; Morris, K.; Law, G. T. W.; Mosselmann, J. F. W.; Bots, P.; Parry, S. A.; Shaw, S. Incorporation and Retention of $^{99}\text{Tc(IV)}$ in Magnetite under High pH Conditions. *Environ. Sci. Technol.* **2014**, *48*, 11853–11862.
- (19) Mayordomo, N.; Rodríguez, D. M.; Rossberg, A.; Foerstendorf, H.; Heim, K.; Brendler, V.; Müller, K. Analysis of Technetium Immobilization and Its Molecular Retention Mechanisms by Fe(II) Al(III) Cl Layered Double Hydroxide. *Chem. Eng. J.* **2021**, *408*, 127265.
- (20) Chotkowski, M.; Czerwiński, A. *Electrochemistry of Technetium; Monographs in Electrochemistry*; Springer International Publishing: Cham, 2021.
- (21) Chotkowski, M.; Czerwiński, A. Electrochemical and Spectroelectrochemical Studies of Pertechnetate Electroreduction in Acidic Media. *Electrochim. Acta* **2012**, *76*, 165–173.
- (22) Chotkowski, M.; Czerwiński, A. Thin Layer Spectroelectrochemical Studies of Pertechnetate Reduction on the Gold Electrodes in Acidic Media. *Electrochim. Acta* **2014**, *121*, 44–48.
- (23) Chotkowski, M.; Wrzosek, B.; Grdeń, M. Intermediate Oxidation States of Technetium in Concentrated Sulfuric Acid Solutions. *J. Electroanal. Chem.* **2018**, *814*, 83–90.
- (24) Paquette, J.; Lawrence, W. E. A Spectroelectrochemical Study of the Technetium(IV)/Technetium(III) Couple in Bicarbonate Solutions. *Can. J. Chem.* **1985**, *63*, 2369–2373.
- (25) Chatterjee, S.; Hall, G. B.; Johnson, I. E.; Du, Y.; Walter, E. D.; Washton, N. M.; Levitskaia, T. G. Surprising Formation of Quasi Stable Tc(VI) in High Ionic Strength Alkaline Media. *Inorg. Chem. Front.* **2018**, *5*, 2081–2091.
- (26) Kuznetsov, V. V.; Chotkowski, M.; Poineau, F.; Volkov, M. A.; German, K.; Filatova, E. A. Technetium Electrochemistry at the Turn of the Century. *J. Electroanal. Chem.* **2021**, *893*, 115284.
- (27) Salaria, G. B. S.; Rulfs, C. L.; Elving, P. J. 456. Polarographic Behaviour of Technetium. *J. Chem. Soc.* **1963**, 2479–2484.
- (28) Salaria, G. B. S.; Rulfs, C. L.; Elving, P. J. Polarographic and Coulometric Determination of Technetium. *Anal. Chem.* **1963**, *35*, 979–982.
- (29) Grassi, J.; Devynck, J.; Trémillon, B. Electrochemical Studies of Technetium at a Mercury Electrode. *Anal. Chim. Acta* **1979**, *107*, 47–58.
- (30) Colton, R.; Dalziel, J.; Griffith, W. P.; Wilkinson, G. 15. Polarographic Study of Manganese, Technetium, and Rhenium. *J. Chem. Soc.* **1960**, 71–78.
- (31) Colton, R.; Peacock, R. D. An Outline of Technetium Chemistry. *Q. Rev. Chem. Soc.* **1962**, *16*, 299–315.
- (32) Astheimer, L.; Schwochau, K. Zur polarographie des technetiums: I. Gleichstrom und wechselstromfolarographische untersuchungen an pertechnetat lösungex. *J. Electroanal. Chem.* **1964**, *8*, 382–389.
- (33) Poineau, F.; Fattahi, M.; Auwer, C. D.; Hennig, C.; Grambow, B. Speciation of Technetium and Rhenium Complexes by in Situ XAS Electrochemistry. *Radiochim. Acta* **2006**, *94*, 283–289.
- (34) Ameer, Z. O.; Husein, M. M. Electrochemical Behavior of Potassium Ferricyanide in Aqueous and (w/o) Microemulsion Systems in the Presence of Dispersed Nickel Nanoparticles. *Sep. Sci. Technol.* **2013**, *48*, 681–689.
- (35) Mayordomo, N.; Rodríguez, D. M.; Schild, D.; Molodtsov, K.; Johnstone, E. V.; Hübner, R.; Shams Aldin Azzam, S.; Brendler, V.; Müller, K. Technetium Retention by Gamma Alumina Nanoparticles and the Effect of Sorbed Fe^{2+} . *J. Hazard. Mater.* **2020**, *388*, 122066.
- (36) Brett, C. M. A.; Brett, A. M. O. *Electrochemistry: Principles, Methods, and Applications*; Oxford University Press, 1993.
- (37) Brett, C. M. A.; Brett, A. M. O. *Electroanalysis*; Oxford University Press, 1998.
- (38) Du, C.; Tan, Q.; Zhang, J. 5—Rotating Disk Electrode Method. In *Rotating Electrode Methods and Oxygen Reduction Electrocatalysts*; Xing, W., Yin, G., Zhang, J. B., Eds.; Elsevier: Amsterdam, 2014; pp 171–198.
- (39) Nightingale, E. R. Viscosity of Aqueous Sodium Perchlorate Solutions. *J. Phys. Chem.* **1959**, *63*, 742–743.
- (40) Andraos, J. On the Propagation of Statistical Errors for a Function of Several Variables. *J. Chem. Educ.* **1996**, *73*, 150–154.
- (41) Bard, A. J.; Parsons, R.; Jordan, J. *Standard Potentials in Aqueous Solution*; Marcel Dekker, Inc.: New York, 1985.
- (42) Wang, X.; Tao, Z. Diffusion of $^{99}\text{TcO}_4^-$ in Compacted Bentonite: Effect of pH, Concentration, Density and Contact Time. *J. Radioanal. Nucl. Chem.* **2004**, *260*, 305–309.
- (43) Ben Said, K.; Fattahi, M.; Musikas, C.; Revel, R.; Abbé, J. C. The Speciation of Tc(IV) in Chloride Solutions. *Radiochim. Acta* **2000**, *88*, 567–571.
- (44) Lafuente, B.; Downs, R. T.; Yang, H.; Stone, N. The Power of Databases: The RRUFF Project. *Highlights in Mineralogical Crystallography*; De Gruyter: Berlin, 2015; pp 1–30.
- (45) Nakamoto, K. *Infrared and Raman Spectra of Inorganic and Coordination Compounds*; John Wiley & Sons, Inc.: Hoboken, NJ, USA, 2008.
- (46) Weaver, J.; Soderquist, C. Z.; Washton, N. M.; Lipton, A. S.; Gassman, P. L.; Lukens, W. W.; Kruger, A. A.; Wall, N. A.; McCloy, J. S. Chemical Trends in Solid Alkali Pertechnetates. *Inorg. Chem.* **2017**, *56*, 2533–2544.
- (47) Thomas, R. W.; Heeg, M. J.; Elder, R. C.; Deutsch, E. Structural (EXAFS) and Solution Equilibrium Studies on the Oxotechnetium (V) Complexes TcOX_4^- and TcOX_5^{2-} (X = Cl, Br). *Inorg. Chem.* **1985**, *24*, 1472–1477.
- (48) Schwochau, K.; Krasser, W. Schwingungsspektren und Kraftkonstanten der Hexahalogeno Komplexe des Technetium(IV) und Rhenium(IV). *Z. Naturforsch.* **1969**, *24*, 403–407.
- (49) Gu, B.; Ruan, C. Determination of Technetium and Its Speciation by Surface Enhanced Raman Spectroscopy. *Anal. Chem.* **2007**, *79*, 2341–2345.
- (50) Mikelsons, M. V.; Pinkerton, T. C. Raman Spectroscopic Evidence for Tc Oxo Cores in Tc HEDP Complexes. *Int. J. Rad. Appl. Instr. A.* **1987**, *38*, 569–570.
- (51) *NIST X ray Photoelectron Spectroscopy Database*, Version 4.1; National Institute of Standards and Technology (NIST): Gaithersburg, USA, 2012.
- (52) Beard, B. C. Sodium Salts of Chlorine Oxyacid Anions, $\text{Cl}(+7)$, Perchlorate, XPS Comparison Spectra. *Surf. Sci. Spectra* **1993**, *2*, 97–103.

Exploring the reduction mechanism of $^{99}\text{Tc(VII)}$ in NaClO_4 : A spectro-electrochemical approach

Diana M. Rodríguez¹, Natalia Mayordomo^{1}, Andrés Parra-Puerto², Dieter Schild, Vinzenz Brendler¹, Thorsten Stumpf¹, Katharina Müller^{1*}*

¹ Institute of Resource Ecology, Helmholtz-Zentrum Dresden – Rossendorf e.V. (HZDR), Bautzner Landstraße 400, 01328 Dresden, Germany.

² Department of Chemistry, Imperial College London, London, SW7 2AZ, United Kingdom.

³ Institute for Nuclear Waste Disposal, Karlsruhe Institute of Technology (KIT), Hermann-von-Helmholtz-Platz 1, 76344 Eggenstein-Leopoldshafen, Germany.

* Corresponding authors: n.mayordomo-herranz@hzdr.de (N. Mayordomo, Phone: +49 351 260 2076), k.mueller@hzdr.de (K. Müller, Phone: +49 351 260 2439)

Content of Supporting Information:

Page SI 2: Figure S1. In-house-built spectro-electrochemical cell

Page SI 3: Figure S2. Reduction curves

Page SI 4: Figure S3. CVs at different scan rates

Page SI 5: Solid analysis

Page SI 6: Figure S4. SEM-EDX

Page SI 7: SI References

Exploring the reduction mechanism of $^{99}\text{Tc(VII)}$ in NaClO_4 : A spectro-electrochemical approach (SI)

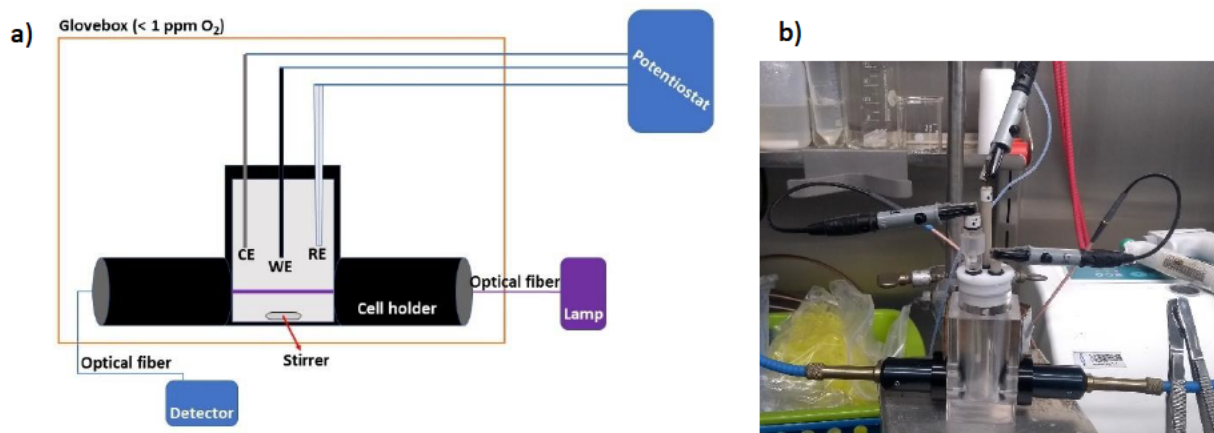


Figure S1. In-house-built spectro-electrochemical cell. a) Schematic representation. b) Real cell inside the glovebox.

Exploring the reduction mechanism of $^{99}\text{Tc(VII)}$ in NaClO_4 : A spectro-electrochemical approach (SI)

Reduction curves

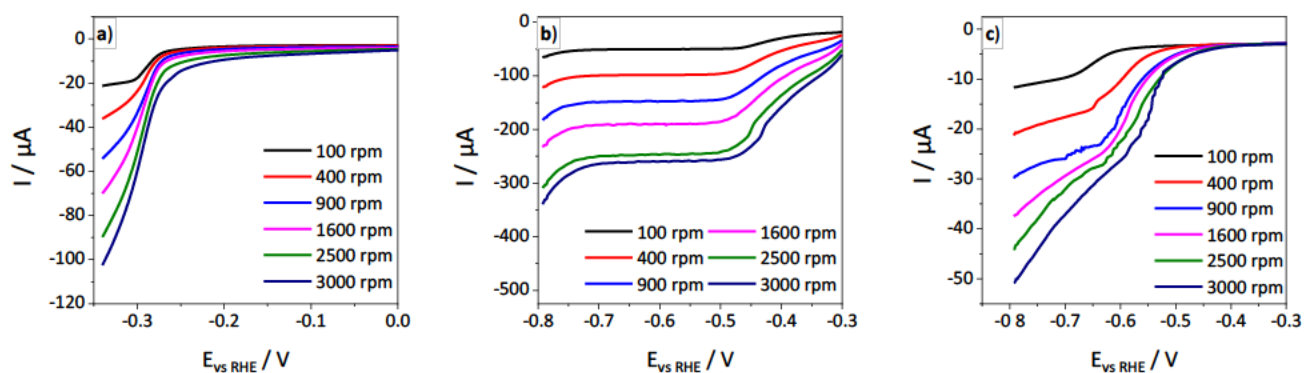


Figure S2. Reduction curves of $0.5 \text{ mM K}_2\text{TcO}_4$ solutions in 2 M NaClO_4 using the RDE a) First cathodic peak at $\text{pH } 2.0$ (-0.318 V vs RHE). b) Second cathodic peak at $\text{pH } 2.0$ (-0.424 V vs RHE). c) Cathodic peak at $\text{pH } 10.0$ (-0.560 V vs RHE). Scan rate: 0.01 V s^{-1}

Exploring the reduction mechanism of $^{99}\text{Tc(VII)}$ in NaClO_4 : A spectro-electrochemical approach (SI)

CVs at different scan rates

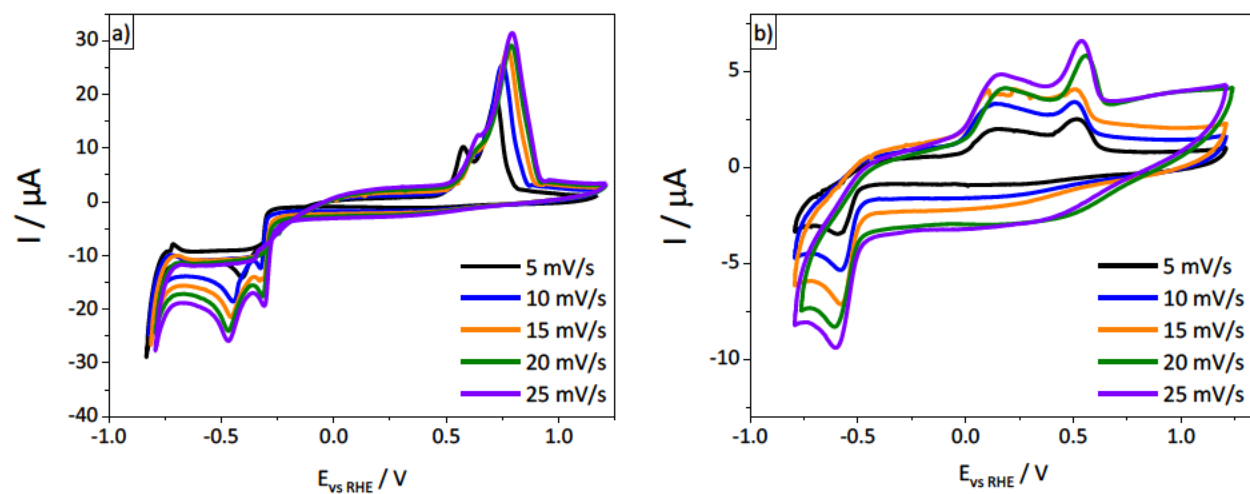


Figure S3. Cyclic voltammograms of $0.5 \text{ mM K}_2\text{TcO}_4$ in 2 M NaClO_4 at different scan rates. a) pH 2.0. b) pH 10.0.

Exploring the reduction mechanism of ⁹⁹Tc(VII) in NaClO₄: A spectro-electrochemical approach (SI)

Solid analysis

Raman microscopy

The dry solid was placed in a Raman cell described elsewhere.¹ To avoid oxygen contact, the cell was sealed inside the glovebox. A Raman microscope (Aramis, Horiba) with a He–Ne laser (wavelength: 532 nm), a 10-fold objective with a D 0.3 filter, a pin-hole of 500 μm and a slit of 600 μm was used to obtain the Raman spectra of the solid samples. Likewise, NaClO₄ and KTcO₄ were measured in solid phase.

X-ray photoelectron spectroscopy

A second batch of the solid at pH 2.0 was produced and shipped to the Institute for Nuclear Waste Disposal at KIT to apply XPS and SEM-EDX. The samples were always transported and measured under inert gas atmosphere (N₂ and Ar).

The solid was mounted on indium foil and moved into the XPS (PHI 5000 VersaProbe II, ULVAC-PHI Inc.) using an airtight transfer vessel. The XPS has a scanning microprobe X-ray source (monochromatic Al K_α (1486.7 eV) X-rays). An electron flood gun generating low energy electrons (1 eV) and low energy argon ions (6 eV) by a floating ion gun were applied for charge compensation at isolating samples (dual beam technique), respectively. The power of the X-ray source is 32 W and 187.85 eV was used as the pass energy of the analyzer to perform survey scans of the samples. Narrow scans of the elemental lines were recorded at 23.5 eV pass energy, yielding an energy resolution of 0.67 eV FWHM at the Ag 3d_{5/2} elemental line of pure silver. The calibration of the binding energy scale of the spectrometer was performed with the binding energies of elemental lines of pure metals (monochromatic Al K_α: Cu 2p_{3/2} at 932.62 eV, Au 4f_{7/2} at 83.96 eV)² yielding an estimated error of ± 0.2 eV. The binding energies of elemental lines were charge referenced to C 1s of adventitious hydrocarbon at 284.8 eV.

Scanning electron microscopy with energy dispersive X-ray spectroscopy

For the SEM-EDX experiments, the samples were mounted to a sample holder and coated with a 20 nm carbon layer inside an anoxic glovebox. The samples were moved with a shuttle (Leica VCT 100) always ensuring inert conditions into the environmental scanning electron microscope (FEI Quanta 650 FEG, now Thermo Fisher Inc.). The pressure in the analysis chamber was 2.8×10⁻⁴ Pa (high vacuum mode) and the operating voltage was 30 kV. SEM-EDX spectra of selected areas were acquired by use of a Thermo Fisher Scientific UltraDry, i.e. Peltier cooled, silicon drift X-ray detector and analyzed by Pathfinder software version 2.8.

Exploring the reduction mechanism of $^{99}\text{Tc(VII)}$ in NaClO_4 : A spectro-electrochemical approach (SI)

SEM-EDX

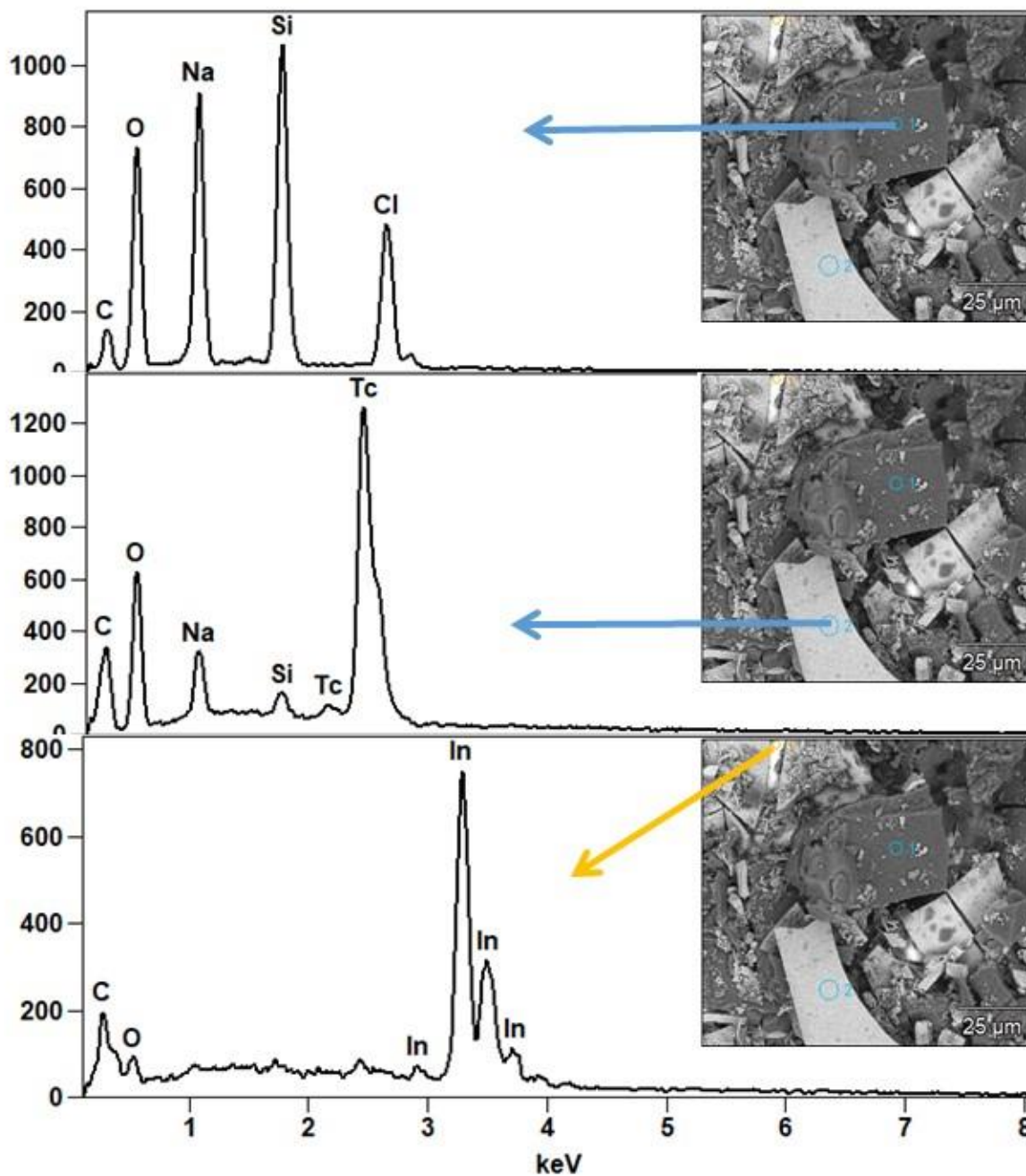


Figure S4. Backscattered electron image showing material contrast and SEM-EDX at selected areas of the solid obtained after the complete reduction of K_7TcO_4 in the spectro-electrochemical cell.

The carbon present in the three regions originates from the carbon coating applied after XPS and before SEM-EDX to avoid surface charging during the measurements while the silicon comes most probably from the dissolution of the quartz cell.

Exploring the reduction mechanism of $^{99}\text{Tc(VII)}$ in NaClO_4 : A spectro-electrochemical approach (SI)

References

- (1) Mayordomo, N.; Rodríguez, D. M.; Schild, D.; Molodtsov, K.; Johnstone, E. V.; Hübner, R.; Shams Aldin Azzam, S.; Brendler, V.; Müller, K. Technetium retention by gamma alumina nanoparticles and the effect of sorbed Fe^{2+} . *J. Hazard. Mater.* **2020**, *388*, 122066.
- (2) Seah, M. P.; Gilmore, I. S.; Beamson, G. XPS: binding energy calibration of electron spectrometers 5—re-evaluation of the reference energies. *Surf. Interface Anal.* **1998**, *26* (9), 642–649.